Microbiological Research 221 (2019) 50–59

Contents lists available at ScienceDirect

Microbiological Research

journal homepage: www.elsevier.com/locate/micres

Enhanced nitrogen and phosphorus activation with an optimized bacterial community by endophytic fungus *Phomopsis liquidambari* in paddy soil

Meng-Jun Tang, Qiang Zhu, Feng-Min Zhang, Wei Zhang, Jie Yuan, Kai Sun, Fang-Ji Xu, Chuan-Chao Dai*

Jiangsu Key Laboratory for Microbes and Functional Genomics, Jiangsu Engineering and Technology Research Center for Industrialization of Microbial Resources, College of Life Sciences, Nanjing Normal University, Nanjing, Jiangsu Province, 210023, China

ARTICLE INFO

Keywords:
Rhizosphere microbiota
Whole developmental stages
Fungal endophyte
Network analysis
Rice
Soil nutrient

ABSTRACT

The endophytic fungus *Phomopsis liquidambari* play a key role in habitat adaptation of rice (*Oryza sativa* L.) with potential multiple beneficial. However, our previous published work on this subject remains incomplete. Here, we performed a soil nutrient (nitrogen and phosphorus) transformation with related functional genes and elucidated how rhizosphere microbiota vary their response to *P. liquidambari* interaction throughout the plant's life cycle under field conditions by Illumina Miseq sequencing platforms in a nutrient-limited paddy soil. Our results showed that *P. liquidambari* symbiosis decreased the nitrogen and phosphorus loss by 24.59% and 17.46% per pot, respectively. Additionally, we suggest that the application of *P. liquidambari* altered the activation of soil nitrogen and phosphorus functional genes to accelerate nutrient turnover in the rice rhizosphere. High-throughput sequencing with co-occurrence network and species-related network analysis further revealed that *P. liquidambari* colonization influenced the patterns of microbiota shift in the rhizosphere, especially during the heading stages. This led to an optimized microbial community through the promotion and inhibition of indigenous soil microbes with a higher level of available nutrient supplies. Our study strongly proposes rice-*P. liquidambari* symbiosis as a useful candidate for improving N and P acquisition and utilization.

1. Introduction

As the most limited nutrients for terrestrial ecosystem productivity, the abundance and behavior of nitrogen (N) and phosphorus (P) in soil has attracted great attention, although their relative importance is generally open to debate (Li et al., 2016). In natural soils, mineral nitrogen and phosphorus in solution usually originate mainly from a high input of chemical fertilizers to avoid organic amendments, which are presumed to be the exclusive form incorporated into a plant's biomass (Bipfubusa et al., 2008). Excessive releases from the soil system into the environment represent large negative consequences to air and water quality such as causing eutrophication and exotic plant invasion, increasing greenhouse gas emissions, and even affecting fundamental aspects of terrestrial ecosystem structure and function (Leip et al., 2015; Belnap et al., 2005).

With increasing concern about agricultural sustainability and environmental protection, recent studies have been dedicated to examining plant-microbial symbiosis, which is an important biotic relationship that can confer profound impacts on host plants by increasing plant nutrient utilization efficiency, strengthening plant tolerance to biotic and abiotic stress, and promoting the accumulation of secondary metabolites (Jia et al., 2016; Talapatra et al., 2017; Yu et al., 2010) that are more cost-effective than chemical fertilizer-based conventional farming. Soil microbe communities perform a crucial role in regulating nutrient fluxes through their involvement in all aspects of C, N, and P cycling in soil and their influence on soil quality and productivity (Anderson et al., 2011; Rashid et al., 2016). It has been reported that endophytic fungus could affect soil microbial ecosystems (Belldereske et al., 2017) and thereby alter biogeochemical cycles mediated by microbes and directly affect the composition of various aspects of soil nutrition.

Phomopsis liquidambari, an endophytic fungus with extensive host range, was originally isolated from the inner bark of *Bischofia polycarpa*. It can form a symbiotic relationship with rice (*Oryza sativa* L.) (Yuan et al., 2007; Yang et al., 2014a), which is a staple food consumed by over half of the world's population. Our previous work unveiled that the

---

Abbreviations: B&D, Broughton and Dilworth; BMM, Bergersen minimal medium; DGGE, denaturing gradient gel electrophoresis; HPLC, high-performance liquid chromatography; ITS, internal transcribed spacer; OD_{600nm}, optical density at 600 nm

* Corresponding author.

E-mail address: daichuanchao@njnu.edu.cn (C.-C. Dai).

https://doi.org/10.1016/j.micres.2019.02.005
Received 13 September 2018; Received in revised form 7 January 2019; Accepted 8 February 2019

rice-*P. liquidambari* interaction not only stimulates genes and regulates phytohormones to improve N absorption in rice (Yang et al., 2014b; Li et al., 2017) but also has the potential to affect the diversity of microbes in the rice rhizosphere soil by altering root exudates and increasing the activities of enzymes (Yang et al., 2015; Siddikee et al., 2016). However, there is a lack of adequate data to determine changes because of technical restrictions (DGGE and PLFA). With the emergence of next-generation sequencing platforms, an exciting tool has emerged in helping us better understand how soil microbes respond to the symbiotic interaction and how they change at both community and taxon levels over time. In addition, increased plant productivity and metabolism with the potential photosynthesis of rice inevitably increases ATP consumption and P uptake; however, to our knowledge, phosphorus inorganic dynamics under *P. liquidambari* symbiosis are not yet well-documented. Moreover, nitrogen (N) and phosphorus (P) have both been demonstrated to limit biomass production in terrestrial ecosystems.

In this context, 16S rRNA gene-based Illumina MiSeq was attempted to obtain a clear picture about the impact of the symbiotic interaction of *P. liquidambari* on the metabolic response of rhizosphere microflora to environmental change in a nutrient-limited paddy soil. Additionally, soil biological processes of nitrogen and phosphorus, including functional genes and nutrient transformation and loss, were measured to uncover potential relationships among microbial guilds, nutrient absorption and crop yield. Based on previous studies, we hypothesize that: (1) there would be a similar trend in nitrogen and phosphorus accumulation of plants and this would consequently inhibit soil nutrient (nitrogen and phosphorus) loss under the application of *P. liquidambari*, (2) *P. liquidambari* symbiosis would accelerate soil nutrient (nitrogen and phosphorus) turnover in the rice rhizosphere by altering the abundance of functional genes, and (3) the abundance and composition of the bacterial community in the rice rhizosphere would be changed by *P. liquidambari* symbiosis with the developmental stage, which may be enhanced by the activation of soil nutrients.

2. Materiel and methods

2.1. Fungal strain and plant seeds

The endophytic fungus *P. liquidambari* was isolated from the inner bark of *Bischofia polycarpa*, labeled with green fluorescent protein (GFP) through a vector plasmid pCT74 by Yang et al. (2014a) and stored on a potato dextrose agar slant (PDA medium, 200 g potato extract, 20 g glucose, and 20 g agar per liter, pH 7.0) at 4 °C. The rice cultivar used in this study was “Wuyunjing 23” (a japonica subspecies of *O.* sativa L.), which is a common cultivar grown in Jiangsu Province, China.

2.2. Inoculation and coculture

P. liquidambari was activated in potato dextrose broth (PDB medium, 200 g potato extract, 20 g glucose per liter, pH 5.5) at 28 °C and shaken at 160 rpm for 3 d and then 10% of the seed culture broth was transferred to new PDB medium under the same conditions for 4 days. In total, 3.51 g (0.387 g dry weight) of fungal mycelia was collected and diluted with 250 mL of sterile distilled water (SDW).

The dehusked rice seeds were surface-sterilized with 70% ethanol for 15 min and bleached in 1.5% sodium hypochlorite for 10 min, which was followed by a thorough rinse in sterilized water. The seeds were then randomly divided into two parts and placed into petri dishes (20 cm diameter and 120 grains per dish). For the endophyte-infected group (E^+), the above-described fungal suspension was added (100 mL per dish). The uninfected group (CK) was treated with an equal amount of SDW as a control. The seeds were germinated in a growth chamber at a controlled condition for 6 days (day/night: 29 °C/25 °C, 16 h/8 h photoperiod at 250 μmol m^{-2} s^{-1}). The rice seedlings were randomly sampled 10 times and checked the infection status of *P. liquidambari* by microscopy to ensure the 100% rate of fungal colonization before transplanting (Supplemental Fig. S1). The colonization of *P. liquidambari* were also detected during the subsequent sample collection in all different stages to ensure the accuracy of the experiment.

2.3. Pot experiment

After germination, identical seedlings were transplanted into pots (25 cm diameter × 30 cm high) containing 15 kg of paddy soil. The paddy soil was yellow-brown loam that was collected from the experimental rice fields (climate: typical subtropical monsoon; annual precipitation: 1107 mm; mean annual temperature: 15.8 °C) in Nanjing Normal University (32° 6.318′ N, 118° 54.88′ E), Jiangsu Province, China. The soil for the experiment was air-dried, mixed to homogeneity, and sieved (2 mm mesh) to remove plant tissues. The physicochemical properties of the soil were as follows: total N, 0.81 g kg^{-1}; available N, 26.23 mg kg^{-1}; total P, 0.53 g kg^{-1}; available P, 16.74 mg kg^{-1}; total K, 0.77 g kg^{-1}; available K, 76.58 mg kg^{-1}; and pH 5.82 according to the method of Niu et al. (2013). After 20 days of growth (mid-June 2017), the seedlings at similar developmental stages were transplanted into pots (4 hills per pot, 1 seedling per hill, and 15 kg soil per pot) and grown in field conditions.

The pot experiments were arranged in a 3 × 2 factorial design with endophyte inoculation (CK, E^+) and three levels of nitrogen applied (the low N was 1.25 g urea per pot, the medium N was 2.5 g urea per pot, and the high N was 3.75 g urea per pot) as the main factors. Phosphorus (1.6 g of P_2O_5 per pot) and potassium (1.4 g of K_2O per pot) were applied as a basal dressing. Each combination was replicated eight times.

2.4. Sample collection

The plants and soil samples were excavated from the pots at 9:30 AM in the seedling stage (S1, June 17, 2017), the tillering stage (S2, July 17, 2017), the grain filling stage (S3, September 7, 2017) and the ripening stage (S4, November 1, 2017), respectively. At every growth stage, six plants were randomly selected from three pots in each treatment (two plants per pot), the grain yield was measured by all of the remaining plants in pots after harvesting. The roots, shoots and seeds (in S4 stage) of plant samples were separated and washed and then used to analyze the height and biomass (70 °C to constant weight) (Supplemental Table S1). The dried samples were then milled to pass through a 1 mm screen for chemical analysis.

Further, after shaking off the loosely adhering soil, the tightly adhering soil on the plant root was carefully collected as rhizosphere soil sample. For each sampling, rhizosphere soil from the same pot were pooled to form one composite sample to obtain three replicates rhizosphere soil samples. The soil samples were air dried and sieved (< 2 mm) immediately after collection, and part of these fresh soil was used for chemical analysis while the other part was stored at −80 °C for DNA extraction.

2.5. Analysis of nitrogen and phosphorus nutrient

To determine the influence of endophyte infection on rice nutrition accumulation, three biological replicates were performed for the nutrient analysis of plants and soil. Fresh rhizosphere soil samples were used to measure the available N (alkali hydrolysis nitrogen) and available P (Olsen P), which can be used directly in crop cultivation, and following the method of the diffusion dish (Inselsbacher and Näsholm, 2012) and Olsen et al. (1954), respectively. The contents of total N and P in the plant (root, shoot and seed) (Supplemental Table S2) and rhizosphere soil (Supplemental Table S3) were measured in accordance with the Kjeldahl method (Hakkeling et al., 1993) and the molybdate colorimetric method (Sommers and Nelson, 1972), respectively. Element conservation principle means the mass of elements remain the same before and after the chemical reaction (Rustad and Cronan, 1988). Based on this principle, the theoretical losses of nitrogen and phosphorus (in gaseous and liquid form) per pot can be estimated by subtracting the total amount (soil and plant) of final nutrition from the total amount (soil and plant) of initial nutrition in each pot (ignore leaching loss).

2.6. DNA extraction and q-PCR

The total DNA was extracted according to the manufacturer's protocols for 400–500 mg of each soil sample with the commercial FastDNA® Spin Kit for Soil (MP Biomedicals, USA). The extracts were characterized by electrophoresis on 1% agarose gels and stored at −20 °C until ready for further processing. To quantify the extracted DNA concentration, the optical density was determined using a UV Spectrophotometer (NanoDrop ND-1000 Technologies, USA) and adjusted to 20 ng μL^{-1}.

To further investigate the ability of nitrogen and phosphorus activation by microorganisms in the rhizosphere soil of rice, we analyzed the functional genes abundance that encodes key enzymes include ammonia monooxygenase (*amoA*), hydroxylamine oxidoreductase (*hao*), nitrite oxidoreductase alpha subunit (*nxrA*), nitrate reductase α subunit (*narG*), nitrite reductase (*nirS*), copper-containing nitrite reductase (*nirK*), nitric oxide reductase subunit B (*norB*), nitrous oxide reductase (*nosZ*); nitrogenase complex (*nifDHK*), dehydrogenase (*gdh*), alkaline phosphatase (*phoD*), polyphosphate kinase (*ppk*), phosphonoacetate hydrolase (*phn*) and phytase (*phyC*) in soil's DNA. Each soil sample was estimated in triplicate by the Real-time PCR Detection System (ABI7500, Applied Biosystems, USA) using the final 20 μl reaction mixtures containing 1 μl template DNA, 10 μl of SYBR Premix Ex Taq (Takara, Shinga, Japan), 0.4 μM of each primer (10 μM) and 8.2 μl sterile water. All of the primers and related references are listed in Supplemental Table S4 and were synthesized by Majorbio Bio-pharm Technology Company (Shanghai, China) and diluted to 10 mmol/L. q-PCR was performed following a three-step thermal cycling procedure: 94 °C (2 min) for one cycle followed by 94 °C (30 s), 60 °C (45 s), and 72 °C (30 s) for 45 cycles. The amplification specificity of the target gene was confirmed by generating a melting curve. The $2^{-\triangle\triangle Ct}$ method (Liu, 2007) was proposed for determining each target gene copy number. β-actin was used as an internal quantitative control and the PCR reaction system was optimized to ensure the amplification efficiencies of each target gene and the reference gene were approximately equal.

2.7. DGGE analysis of soil bacterial community

The bacterial community structure of the whole growth period of the communities in the soil samples were clustered by denaturing gradient gel electrophoresis (DGGE) analysis as described in Kan et al. (2006). The bacterial 16S rRNA gene fragments of the rice rhizosphere soil were amplified in triplicate with primers set of 518r(5′-GTATTAC CGCGGCTGCTGG-3′)/GC-341f(5′-CGCCCGCCGCGCGCGGCGGGCGGG GCGGGGGCACGGGGGGCCTACGGGAGGCAGCAG-3′) using an Eppendorf C1000 Touch Thermal Cycler (Eppendorf, Hamburg, Germany) for PCR-DGGE analysis. The 50 μL reaction mixtures consisted of 5 μL of 10 × Taq PCR buffer (containing Mg^{2+}), 4 μL of 2.5 mM dNTPs, 1 μL of 10 mM of each primer, 1 μL of Taq DNA polymerase (Takara, Japan), and 1 μL of DNA extract. The touchdown PCR strategy was as follows: initial denaturation at 94 °C for 5 min and a touchdown procedure (94 °C for 1 min, annealing for 50 s at temperatures decreasing from 65 to 55 °C during the first 20 cycles, and ending with an extension step at 72 °C for 1 min); followed by 20 cycles of 94 °C for 1 min, 55 °C for 50 s, 72 °C for 1 min; and final extension at 72 °C for 10 min and cooling at 4 °C. The PCR products were checked by 1% (w/v) agarose gel electrophoresis.

The DGGE analyses were performed with a DCode universal mutation detection system (Bio-Rad, USA) as follows: a 30 μL PCR amplicon of bacteria was deposited in each well and separated on an 8% (w/v) polyacrylamide (acrylamide:acrylamide = 37.5:1) gel with a 40–70% denaturant gradient (the 100% denaturant contained 7 mol L^{-1} urea and 40% formamide) and then run in a 0.5 × TAE (Tris-acetate-EDTA) buffer at 80 V and 60 °C for 16 h. For comparative purposes, three amplification of soil samples for each treatment were randomly chosen to displayed on the DGGE gel-sheet. After electrophoresis, the gels were stained with EB for 20 min and then photographed under a GelDOC-ItTS imaging system (Ultra Violet Products, Upland, CA, USA).

Gelcompar II (Applied Maths, Austin, TX, USA) was used to analyze the DGGE profile information on individual gels, and cluster analysis was performed to construct a dendrogram using the unweighted pair group method (UPGMA) based on Pearson's similarity coefficient. Principal Component Analysis (PCA) was performed by SPSS 20.0 (IBM SPSS Statistics, Armonk, NY, USA) and using relative band peak area intensity data from the Gelcompar II results.

2.8. Illumina Miseq sequencing and analysis

According to the PCA-clustering of DGGE analysis, Illumina Miseq sequencing was performed for soil samples under low N condition to facilitate an in-depth in dissection of the effects of endophytic fungi on rhizosphere microorganisms by the Illumina MiSeq PE300 platform at Majorbio Bio-pharm Technology Co., Ltd. (Shanghai, China). There are three biological replicates for each treated soil sample to alleviate environmental bias. Primers 338 F (5′-barcode-ACTCCTACGGGAGGCAG CAG-3′) and 806R (5′-GGACTACHVGGGTWTC TAAT-3′) were used to amplify the V3-V4 regions of the bacterial 16S rRNA gene (Gene Amp 9700, ABI, USA), then the forward and reverse reads merged prior to data analysis.

The sequences were quality-filtered using the Quantitative Insights into Microbial Ecology (QIIME) pipeline software (http://qiime.org/tutorials/tutorial.html) and low quality reads were removed by Trimmomatic. The qualified sequences were clustered into operational taxonomic units (OTUs) at the 97% identity threshold using the Usearch program (version 7.1). The taxonomic classification of OTUs was annotated with the Ribosomal Database Project (RDP) classifier (http://rdp.cme.msu.edu/), and the obtained data was used for subsequent analyses. The rarefaction curves (RC), indices of bacterial community richness (Chao 1, ACE) and diversity (Shannon and Simpson) of the Illuminance MiSeq data were conducted in the Mothur software package (version 1.27.1) (http://www.mothur.org/wiki/454_SOP) (Schloss et al., 2009). Network X software of the Python package (Klarner et al., 2017) was used to build and train the co-occurrence network and the species-related network to show a visual expression of species abundance information among different samples.

Other analyses, such as the principal coordinate analysis (PCoA), redundancy analysis (RDA), heatmap and Mantel test, were implemented using vegan package (Oksanen et al., 2013) R version 3.20 environment (the R Foundation for Statistical Computing, Vienna, Austria). The raw sequences in this study have been deposited in the NCBI Sequence Read Archive (SRA) database under the accession number SRP 149303.

2.9. Statistical analyses

The basic statistical analyses were conducted as a one-way ANOVA with different treatments (CK vs. E^{+}) under the same level of N by SPSS 20.0 (IBM SPSS Statistics, Armonk, NY, USA). All of the experiment data in this study are shown as the means and standard errors (SE) resulting from at least triplicate analyses, which were considered as significantly different at $*P < 0.05$ and $**P < 0.01$ by Tukey's test. Other statistical analyses and drawings were plotted by Origin 8.0 (Microcal Software, Northampton, MA).

3. Results

3.1. Rice growth dynamics and yield

Generally, the fungus-infected plants showed significantly higher height and biomass than those of uninfected plants under low N (Supplemental Table S1). The total height of the coculture plant was increased by 7.03%, 5.05%, 3.48%, and 4.55% and the total biomass was increased by 12.57%, 14.49%, 8.53% and 7.08% at four growth stages, respectively, compared to the untreated group. However, the favorable effect of endogenous fungi was weakened in the middle N condition, which significantly increased the height of the plant shoot and root but had little promotion of the biomass. In addition, *P. liquidambari* infection did not induce significant changes under the high N levels.

The parameters of grain yield (Supplemental Fig. S1) presented the same rules of growth dynamics. Under low N application, there were higher numbers of panicles per plant (18.49%), filled grains per panicle (6.13%), seed-setting rate (3.52%) and 1000-grain weight (7.66%), which was caused by infection, whereas there was no apparent significant effects on the grain yield under middle N and high N.

3.2. Theoretical amount of nitrogen and phosphorus loss in the pot

Compared to the control, *P. liquidambari* significantly increased the initial and final nitrogen accumulation of plants in the low N application by 27.14% and 12.03%, respectively (Fig. 1b and d). By subtracting the total nitrogen of soil and plant (final, Fig. 1c-d) from the total nitrogen of the soil and plant (initial, Fig. 1a-b), the theoretical nitrogen spillover (gaseous form loss, generally considered as powerful greenhouse gas (NOx)) under *P. liquidambari* infection was decreased 24.59% per pot (Fig. 1e) in low N condition. Under middle N and high N levels, *P. liquidambari* infection did not induce significant changes.

Interestingly, similar but limited trends were observed in Fig. 1(f–j). As we predicted, phosphorus accumulation of the plant under *P. liquidambari* symbiosis were higher at the initial and final stage by 21.09% and 14.9%, respectively (Fig. 1g and i). However, the total soil P concentrations were unaffected by N fertilization when examining all treatments combined (Fig. 1f and h). Approximately 17.46% less phosphorus loss occurred in the infected group per pot under low N comdition, which usually leaches into lakes and causes eutrophication, and there was no apparent endophyte effect under miiddle N and high N (Fig. 1j). These results suggested that the *P. liquidambari* treatment enhanced the absorption efficiency of plant and caused a substantial decrease in nutrition (nitrogen and phosphorus) loss under low N inputs.

3.3. Responses of microbial-specific functional genes to P. liquidambari

Based on the q-PCR results, the *P. liquidambari* treatment had a positive effect on the abundance of *amoA*, *hao* for $NH_4{}^+$-$NO_2{}^-$ transformation and *nosZ*, *nifHKD* for N_2O-$NH_4{}^+$ transformation, but a negative effect on the abundance of *nirS* and *nirK* for NO_2–NO transformation in low N application (Fig. 2A, Supplemental Table S5). Nevertheless, no significant effect was recorded for the abundance of the *nxrA*, *narG*, *napA* (NO_2–NO_3–NO_2- transformation) and *norB* (NO-N_2O transformation) gene between the two treatments (CK vs. E^+). This result may be indicative of a increase in nitrating and nitrogen fixing activity, but a decrease in denitrifying activity under the LN treatments with endophytic colonization of *P. liquidambari*.

Remarkably, the abundances of the four key functional genes (*ppx*, *ppk*, *phoD*, and *phyC*) associated with phosphorus cycling remained stable under all fertilization treatments (Fig. 2B, Supplemental Table S6). However, the endophyte treatment soil led to a higher available phosphorus supply under three N fertilizer levels (Supplemental Table S3), which indicates that the mechanisms of phosphorus activation in the rice rhizosphere soil by fungal endophyte symbiosis was different from nitrogen.

3.4. DGGE-PCA analysis of soil bacterial community

In terms of the bacterial communities composition, the band-clustering analysis of PCR-DGGE indicated that the *P. liquidambari* symbiosis (E^+) treatments showed low similarity with control (CK) treatments under low N condition at both S2 and S3 stage, but the band patterns of other treatments were clustered together under middle N and high N condition (Fig. 3A). which meant the effects of *P. liquidambari* on bacterial communities normally occurred under a low-N level.

3.5. Composition of soil bacterial community by Illumina Miseq sequencing

In total, maximal information was performed based on the 5269 OTUs obtained from the low N soil samples with 50936 high-quality sequences per sample (ranging from 46,598 to 58,218 sequences) by Illumina Miseq sequencing, The good's coverage was on average 97.33 ± 0.32% and the rarefaction curves showed clear asymptotes (Supplemental Fig. S3 and Table S7), which both demonstrate an adequate sequencing depth for a reliable analysis of the soil microbial group.

As shown in Fig. 3B (Supplemental Table S8), the co-occurrence patterns of bacterial OTUs between the vegetative stages (S1: seeding and S2: tillering) and reproductive stage (S3: heading and S4: ripening) in the control samples were homogenous, whereas the composition in the four periods of the *P. liquidambari* infection group were separate from each other. Similarly, the PCoA analysis (Fig. 3C, Supplemental Table S9) and cluster analysis (Fig. 3D, Supplemental Table S10) of community composition based on the Illumina Miseq sequencing implied that a number of OTUs differed in composition between endophyte treatment and the control.

3.6. Heatmap analysis

The 100 most abundant genera in each treatment were clearly revealed by heatmap analysis (Fig. 4, Supplemental Table S11) and their abundances were represented by the average of three replicates to minimize the disparity between samples. Although differences in the bacterial phylogenetic composition were minor among all of the treatments at first sight, those in some typical taxa were obvious between the two treatments. For instance, the relative abundance of *Brevibacillus* and *norank_c_Acidobacteria* (which were affiliated with the phyla *Firmicutes* and *Acidobacteria*, respectively) decreased with time, which were generally considered to be the beneficial microorganisms that related to the effective activation of soil phosphorus (Martínez et al., 2015; Qiu et al., 2012), whereas *P. liquidambari* treatments had higher relative abundances compared to the control during the same stage.

Similar trends were also observed in the *norank_f_Nitrosomonadaceae*, *Bradyrhizobium* and *Nitrospira* families (which are affiliated with the phyla *Proteobacteria* and *Nitrospirae*, respectively), considering that most members of these families have been reported to be able to fix and nitrify N (López et al., 2018; Kraigher and Mandic, 2011). In contrast, the *Acinetobacter* and *Achromobacter* families (affiliated with the phyla *Proteobacteria*), which might cause soil denitrification (Su et al., 2016; Youatt, 1954), exhibited lower relative abundances in endophyte treatments than in the control. Overall, endophyte symbiosis provide a different relative abundance of the indigenous soil microbes with a higher nutrient (nitrogen and phosphorus) supply.

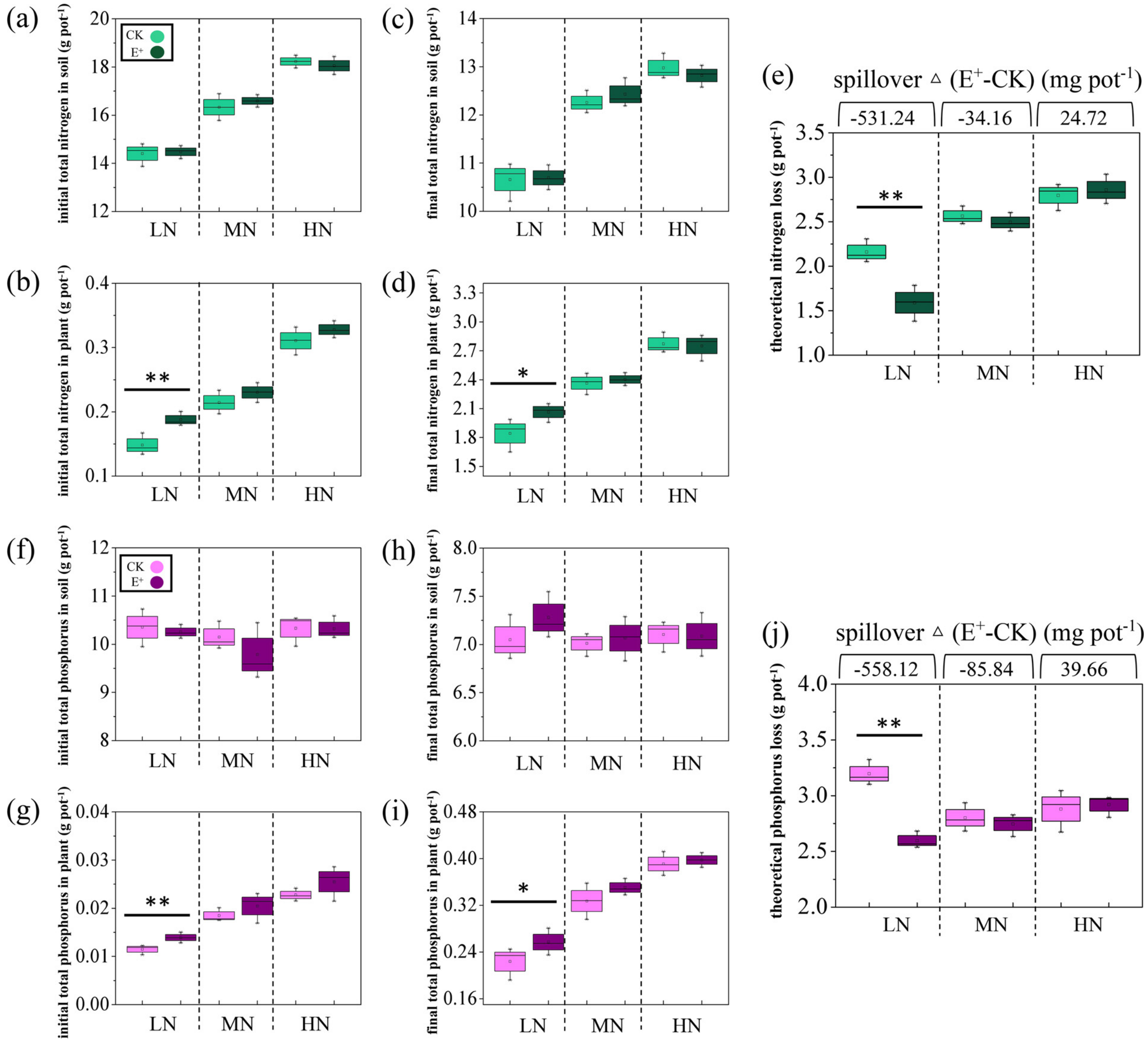

Fig. 1. Effect of *P.liquidambari* infection on the loss of soil nitrogen (a–e) and phosphorus (f–j) in each pot under different N levels. (a) the initial total nitrogen in soil; (b) the initial total nitrogen in plant; (c) the final total nitrogen in soil; (d) the final total nitrogen in plant; (e) the theoretical nitrogen loss in each pot; (f) the initial total phosphorus in soil; (g) the initial total phosphorus in plant; (h) the final total phosphorus in soil; (i) the final total phosphorus in plant; (j) the theoretical phosphorus loss in each pot. Each value represents mean ± SE, n = 3. **P* < 0.05; ***P* < 0.01 (t-test). LN-low nitrogen, MN-middle nitrogen, HN-high nitrogen, CK, endophyte-uninfected, E^+ endophyte-infected.

3.7. *Structure and network of the soil microbial communities*

The structure of the microbial communities between two treatments were compared at the phylum level in Fig. 5A (Supplemental Table S12). The dominant bacterial phyla with sequence percentages across all samples were *Proteobacteria*, *Chloroflexi*, *Actinobacteria*, *Firmicutes*, *Acidobacteria*, and *Bacteroidetes* with relative abundances ranging from 25.14% to 34.27%, 9.76% to 22.29%, 11.57% to 18.38%, 3.89% to 14.38%, 5.68% to 13.71%, and 3.20% to 12.46%, respectively. Morever, *Gemmatimonadetes*, *Cyanobacteria*, *Nitrospirae*, *Verrucomicrobia*, and *Armatimonadetes* were found at low abundances in all of the samples and comprised 1.46% to 3.54%, 1.17% to 2.89%, 0.72% to 2.24%, 0.58% to 1.63%, and 0.38% to 1.30% of the community, respectively.

The species-related network analysis was usually used to perform a determination of the co-existence of species in environmental samples. Fig. 5B (Supplemental Table S13) showed the visual correlation between soil microbial communities at the phylum level in the heading stage. For comparability, we used *Chloroflexi* (purple node) as a reference, which is a facultative anaerobe with continuous increased abundance during the growing period. Remarkably, *Chloroflexi* (purple node) was negatively correlated with *Acidobacteria* (blue node) and *Nitrospirae* (orange node) (Fig. 5B-1) in control rhizosphere, but positively correlated with them under *P. liquidambari* infection (Fig. 5B-2). This indicated that the *Acidobacteria* and *Nitrospirae*, which are generally considered to be beneficial microorganisms in soil, have an increasing trend during this stage.

3.8. *Relationship between the bacterial community and soil characteristics*

Redundancy analysis (RDA) ordination plots revealed a marked correlation between the bacterial community and soil proprieties (Fig. 6, Supplemental Table S14), which were determined by a 999 Monte Carlo permutation-based significance test. After removal of the redundant variables, six environmental characteristics (TN, TP, AN, AP, pH, and N/P) were chosen for RDA. The first two RDA axes explained 24.50% and 6.73% of the total variation in the data.

Among the six variables tested, N/P (r^2 = 0.2068, $P > 0.01$) was the only factor that did not significantly contribute to the bacterial

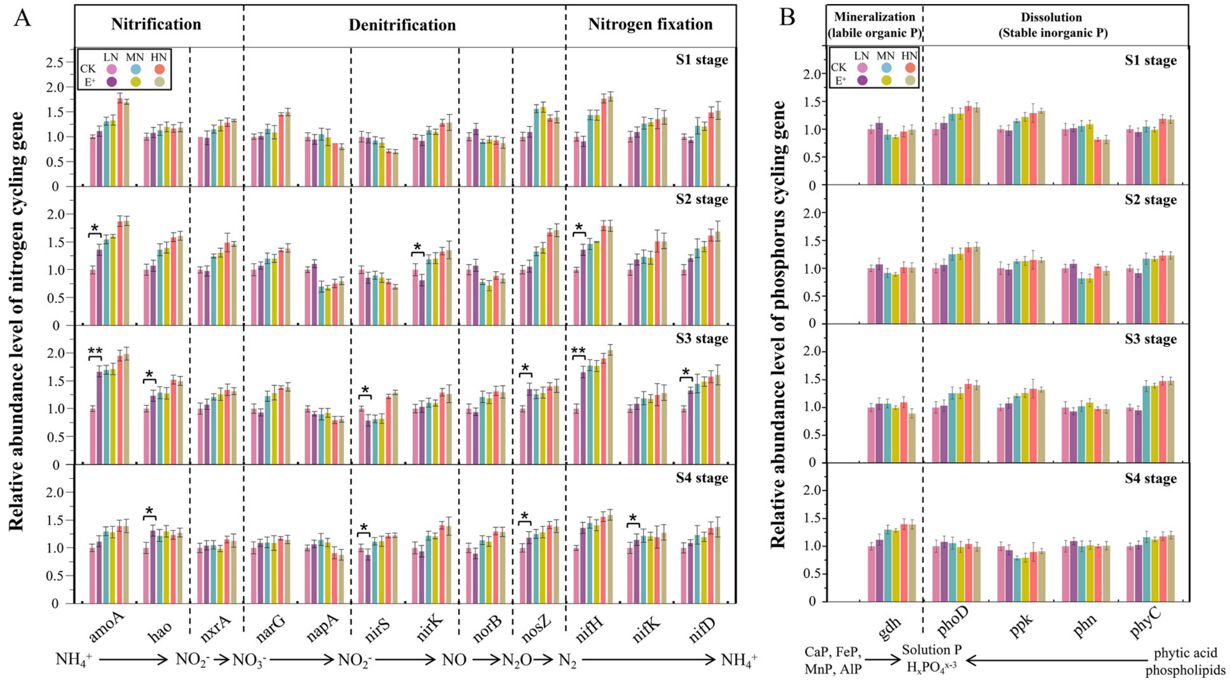

Fig. 2. Effect of *P.liquidambari* infection on the abundance of nitrogen (A) and phosphorus (B) cycling-related genes in the rice rhizospheric soil. ammonia monooxygenase (*amoA*), hydroxylamine oxidoreductase (*hao*), nitrite oxidoreductase alpha subunit (*nxrA*), nitrate reductase α subunit (*narG*), nitrite reductase (*nirS*), copper-containing nitrite reductase (*nirK*), nitric oxide reductase subunit B (*norB*), nitrous oxide reductase (*nosZ*); nitrogenase complex (*nifDHK*), dehydrogenase (*gdh*), alkaline phosphatase (*phoD*), polyphosphate kinase (*ppk*), C-P lyase (*phn*) and phytase (*phyC*). Gene abundance were compared between samples in same nitrogen fertilizer level. S1:seeding stage; S2:tillering stage; S3:heading stage, S4:ripening stage. Each bar represents mean ± SE, n = 3. *$P < 0.05$; **$P < 0.01$ (t-test). LN-low nitrogen, MN-middle nitrogen, HN-high nitrogen, CK, endophyte-uninfected, E^+ endophyte-infected.

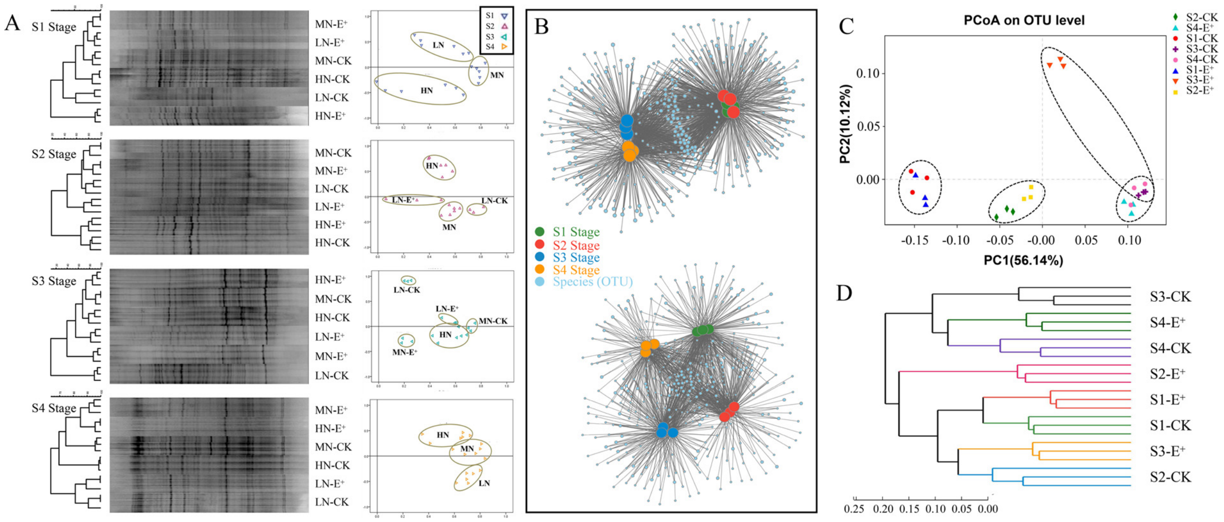

Fig. 3. Comparison of the bacterial community structures at four growthing stage of rice rhizosphere soil, n = 3. (A) DGGE profile under different N levels; (B) Co-occurrence network analysis. The closer distance of the sample nodes represent higher species similarity. (C) Principal coordinates analysis (PCoA) based on weighted UniFrac distances and (D) Hierarchical clustering tree based on OTU under low N level. S1:seeding stage; S2:tillering stage; S3:heading stage, S4:ripening stage. LN-low nitrogen, MN-middle nitrogen, HN-high nitrogen, CK, endophyte-uninfected, E^+ endophyte-infected. The nodes in the network represent the sample nodes (big in four colors) and the species nodes (small in light blue), the closer between sample nodes, the higher similarity.

community composition, whereas TN ($r^2 = 0.4121$, $P = 0.003$), TP ($r^2 = 0.5191$, $P = 0.002$), AN ($r^2 = 0.5196$, $P = 0.001$), AP ($r^2 = 0.5959$, $P = 0.001$), and pH ($r^2 = 0.5767$, $P = 0.001$) significantly affected the bacterial community structure regardless of the analysis methods. Furthermore, our results showed that samples from the endophyte treatment (E^+) were most negatively influenced by TN, TP, AN, AP and pH, whereas samples from the control treatment were most positively influenced by these variables, which indicated that the effect of *P. liquidambari* inoculation on microbial communities may primarily be mediated by soil chemical characteristics.

4. Discussion

4.1. Impacts of P. liquidambari on crop absorption and nutrition loss

Harnessing the plant-microbiota symbiotic interactions can assist in sustainably increasing primary productivity to meet growing global demands for food (Ban et al., 2017). In this study, our results

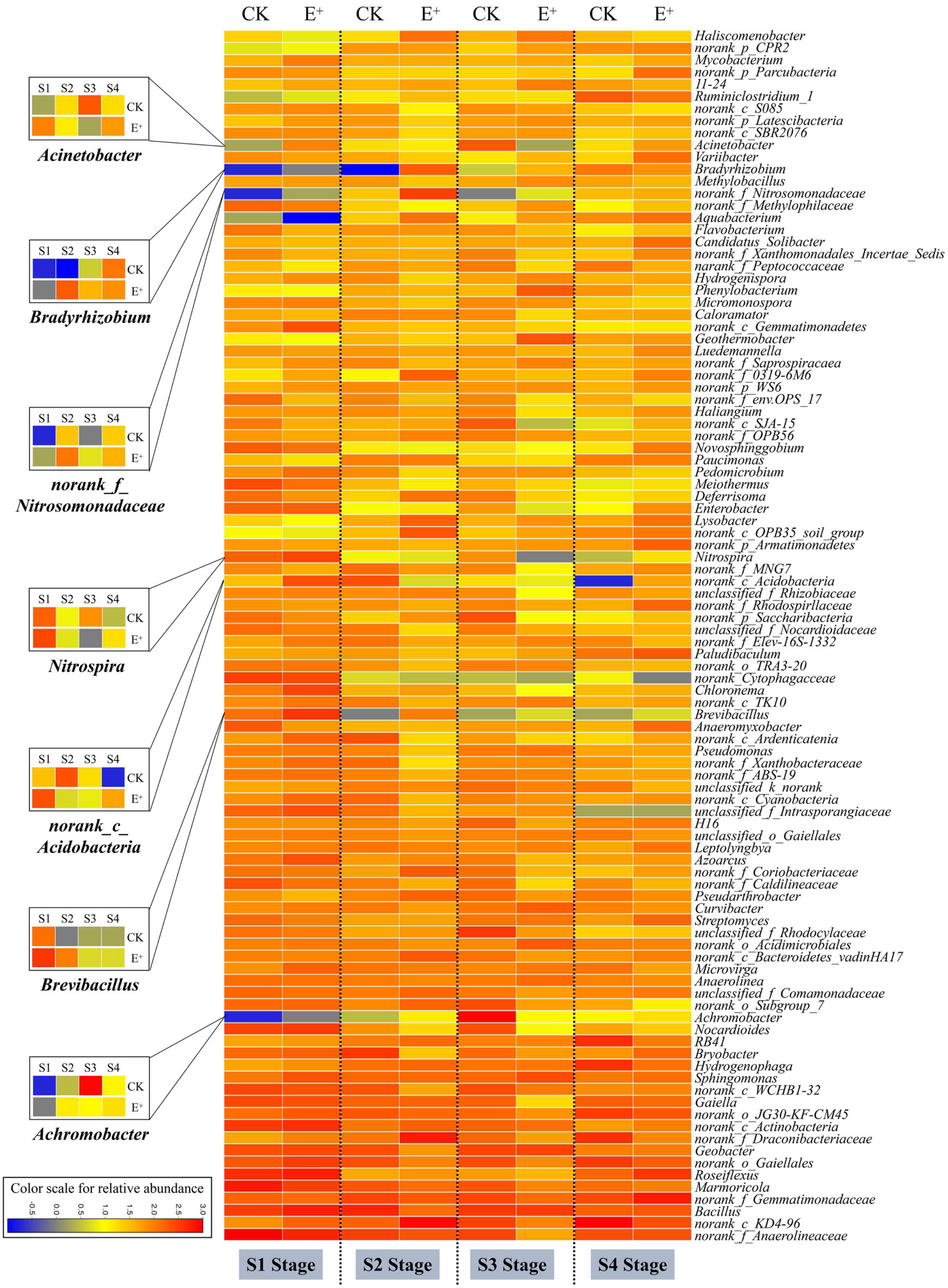

Fig. 4. Distribution heatmap of the top 100 microbial genera in rice rhizosphere soil with different stage of rice growing under low N level. S1: seeding stage; S2: tillering stage; S3: heading stage, S4: ripening stage, CK, endophyte-uninfected, E^+ endophyte-infected. Red colors indicate higher abundance; blue and yellow colors indicate lower abundance. Each bar represents average relative abundance of three replicates.

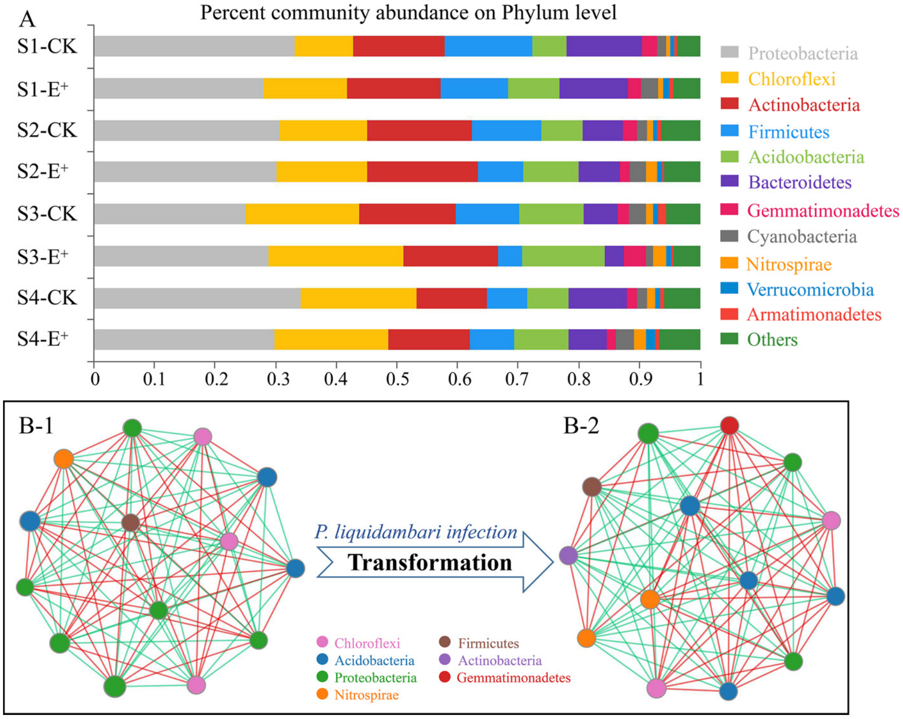

Fig. 5. (A) Average relative (n = 3) abundance of bacteria community for each sample and (B) Species-related network analysis at phylum level during heading stage based on Spearman's rank correlation coefficients. S1: seeding stage; S2: tillering stage; S3: heading stage, S4: ripening stage, CK, endophyte-uninfected, E^+ endophyte-infected. Node size reflects the node degree (number of neighbours/correlations in the network). Red line indicates the positive correlation between species, and green line indicates the negative correlation between species in network map.

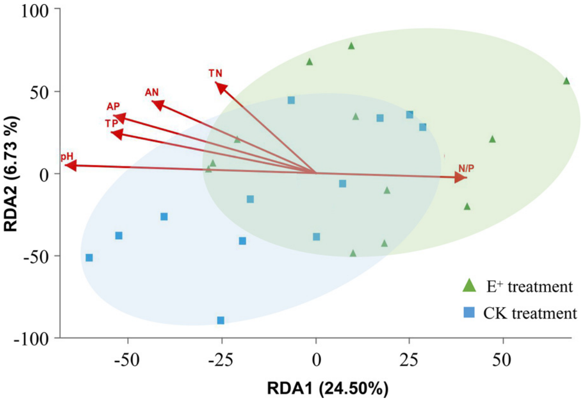

Fig. 6. Redundancy analysis (RDA) of bacterial community and soil characteristics (arrows) at phylum level, n = 3. CK, endophyte-uninfected, E^+ endophyte-infected. TN, total nitrogen; AN, available nitrogen; TP, total phosphorus; AP, available phosphorus (Olsen phosphorus); N/P: ratio of total nitrogen to total phosphorus.

demonstrated that *P. liquidambari* had beneficial effects on plant growth and yield (Table S2 and Fig. S2). The beneficial effects of *P. liquidambari* infection on rice plants tended to attenuate with the increasing concentrations of applied N-fertilizer. These findings were in line with previous work suggesting that treatment with the *P. liquidambari* could significantly promote rice host growth and yield in a nitrogen-limited condition (LN level) (Yang et al., 2014b; Li et al., 2017). Likewise, this was also supported by Khan et al. (2015) who found that the endophytic fungus *Fusarium tricinctum* RSF-4 L and *Alternaria alternata* RSF-6 L, which were isolated from the leaves of *Solanum nigrum,* could synthesize bioactive compounds (indole acetic acid) and significantly promote plant growth.

Fertilization was a crucial management practice used to raise crop productivity in paddy soil for its severely poor in nutrients (Nie et al., 2010). Our results confirmed that the fungal endophyte had a role in promoting the nutrition accumulation of rice and elevating soil available nutrient levels in the rhizosphere soil (Table S3 and S4).

Additionally, because the pot experiment was conducted outdoors, there were certain deviations in the nutrition loss calculation for the nutrient change caused by rainfall or runoff. However, our calculation of each pot was near the same baseline with almost equal loss and the trends shown in the calculation results were reliable. The *P. liquidambari* treatment reduced the loss of nitrogen and phosphorus in a closed pot experiment by enhancing the nutrient absorption efficiency of the crop (Fig. 1), which highlights the potential of the fungal endophyte to achieve a balance in maximizing crop yields and in minimizing nutrient pollution associated with the application of fertilizer.

4.2. Impacts of P. liquidambari on microbial-specific functional genes

Previous studies of the inorganic nitrogen dynamic response to the plant-*P. liquidambari* interaction have notably focused on N_2 fixation and the nitrification processes and related microbes (Yang et al., 2015), however, as a large contributor to agricultural NO emissions (denitrification in rice cultivation) cannot be ignored, and the micro-hypoxia environment created by the immersed plant roots is conducive to the reproduction and adhesion of denitrification bacteria (Wang et al., 2015).

In this study, we mainly focused on relative abundance changes of soil functional genes, may not be optimal compared with absolute quantitation, but should be sufficient to draw a conclusion that the soil nitrogen activation functional genes were altered by *P. liquidambari* symbiosis (Fig. 2A). Our result confirmed that *P. liquidambari* symbiosis significantly inhibited partial denitrification process in the rhizosphere soil and reduced the gaseous loss of N-fertilizer, which was probably due to the increase in the oxygen secretion of the symbiosis plant roots (data unpublished), whereas the promotion of nitrogen fixation and nitrification was consistent with previous studies. Similarly, such findings were consistent with the data concentrated on distribution and activity of soil functional microorganisms, which mostly revealed only a single number of functional groups such as methanotrophs (Xu et al., 2017), denitrifiers (Yoshida et al., 2010), and the ammonia-oxidizing bacteria and archaea (Wei et al., 2011) community.

Furthermore, the mobilization of phosphorus was not limited by fertilizer according to the conclusion shown in Fig. 2B. It is tempting to speculate that *P. liquidambari* may enter the soil through decayed root tissue at later stages (Supplemental Fig. S4a) given their endophytic and saprophytic systems with rice (Zhou et al., 2017) and showed highly efficient phosphorus (lecithin, tricalcium phosphate and phytate) solubilization in rhizosphere soil (Supplemental Fig. S4b-d), which resulted in a significant increase in available phosphorus in the soil. Thereby, *P. liquidambari* showed great potential to promote nutrient transformation in root soil through this symbiotic interaction. However, the effect of fungi on the nutrient absorption and transport of aboveground plant tissues needs to be demonstrated in future studies.

4.3. Impacts of P. liquidambari on the shift pattern of the soil bacterial community

Land plants usually form intimate relationships with the diverse root microbiome distinct from the microbial community present in surrounding soil (Fitzpatrick et al., 2018). The qualitative and semi-quantitative information about bacterial taxonomic compositions and abundances of the rhizosphere communities at different growth stages between two different treatments (CK vs E^{+}) were assessed by PCR-DGGE and Illumina Miseq sequencing, respectively. High-throughput sequencing revealed that the untreated samples maintained a relatively stable microbial community, whereas *P. liquidambari* symbiosis could lead to temporary changes in the structure and composition of soil bacteria during the S2 (tillering) and S3 (heading) stages, but this effection gradually disappeared in the S4 (ripening) stage (Fig. 3B and C), which was mostly consistent with the clustering analysis of PCR-DGGE. In summary, the various clustering methods implied a same rusult that the colonization by the fungal endophyte *P. liquidambari* caused changes in the rhizosphere microbiota shift pattern. However, a recent study presented a different time-series shift by Zhang et al. (2018) who found that the rice root microbiota varied dramatically during the vegetative stages and stabilized from the beginning of the reproductive stage until rice ripening, which might be determined by both the geographic location and the plant genotype (IR24 and *Nipponbare*).

4.4. Impacts of P. liquidambari on the soil bacterial community with nutrient activation

During the field conditions, the root microbiota community of rice has a dynamic pattern of gradually deteriorating, especially the reduction of *Nitrospira*, which is related to the facilitation of nitrate assimilation. Nevertheless, *P. liquidambari* symbiosis slowed the rate of soil deterioration compared to the controls (Fig. 4). These results differ from the results showing that *Nitrospira* started to accumulate in the rice root at the tillering stage and remained at a high level during the rice reproductive stage to provide advantages for rapid growth (Ding et al., 2018). The difference probably occurred because the paddy soil investigated in this study was flooded when sampling, and the anoxic conditions were not conducive to the nitrification process. According to these dynamic changes, *P. liquidambari* symbiosis contributed to shaping the bacterial community structure and permitted a better functional level of nitrogen and phosphorus turnover through the promotion and inhibition of various indigenous soil microbes, which was mostly consistent with the data in Supplemental Table S4.

4.5. Impacts of P. liquidambari on the composition and structure of the soil bacterial community

Our microbial compositions (Fig. 5A) agreed with numerous previous studies (Edwards et al., 2015; Hardoim et al., 2011) which suggested that *Proteobacteria*, *Chloroflexi*, *Actinobacteria*, *Firmicutes*, *Acidobacteria*, and *Bacteroidetes* might be the predominant phylum in paddy soils. Furthermore, we showed visual species-related networks that demonstrate the optimization of the interaction in the microbial community (Fig. 5B) for the first time. These findings further indicated that *P. liquidambari* application might accelerate soil nutrient turnover by improving the coexistence of species with the development of the soil microbial community structure, which was consistent with our early published study that *P. liquidambari* could increase the structural and functional diversity of microbes in the same paddy soil (Siddikee et al., 2016), as this study used Illumina Miseq.

As a ‘seed bank’ of microorganisms, biotic and abiotic factors in soil always determines the structure and function of microbial communities in the rhizosphere (Berg and Smalla, 2010; Liang et al., 2018). In this study, the effect of *P. liquidambari* inoculation on microbial communities may primarily be mediated by soil chemical characteristics (Fig. 6). We speculated that colonization by the fungal endophyte *P. liquidambari* in rice provided a betterment biotope for most indigenous soil microbes through alteration of the rhizosphere micro-environment, an interface of nutrition exchange between plant roots and soil, such as the exudates and oxygen secretion of symbiosis plant roots, or self-secreting substances (Zhalnina et al., 2018), which perhaps were the essential reasons for the improved supply of nutrients available for plants in the soil under low N conditions. Further investigations will reveal the mechanism underlying this specific microbial regulation process.

5. Conclusions

A growing amount of evidence indicates that endophytic fungi is integral to host plant function including growth and fitness (Bizabani and Dames, 2015; Jia et al., 2016), yet our understanding of their broader ecological importance remains limited. Our study provides evidence of the active interconversion of organic and inorganic nutrition (nitrogen and phosphorus) forms in the soil, as well as this cycling activity is catalyzed via optimizing the structure of the root microbiome in nitrogen-limited (low N application) soil with *P. liquidambari* treatment. This study may also a good complement and improvement to our previous series of published studies. Our findings inform future efforts to learn the process of the rice root microbiota establishment and reemphasize the important role played by plant-*P. liquidambari* symbiosis to increase plant performance in the face of deprivation nutrition.

Conflicts of interest

No conflict of interest to declare.

Acknowledgements

This work was supported by the National Natural Science Foundation of China (NSFC NO. 31570491), the National Key Research and Development Program (NO. 2017YFDO800705), the Priority Academic Program Development (PAPD) of Jiangsu Higher Education Institutions of China and the Jiangsu Agriculture Science and Technology Innovation Fund CX(17)-1001 (JASTIF,CX(17)1001).

Appendix A. Supplementary data

Supplementary material related to this article can be found, in the online version, at doi:https://doi.org/10.1016/j.micres.2019.02.005.

References

Anderson, C.R., Condron, L.M., Clough, T.J., Fiers, M., Stewart, A., Hill, R.A., Sherlock, R.R., 2011. Biochar induced soil microbial community change: implications for biogeochemical cycling of carbon, nitrogen and phosphorus. Pedobiologia 54, 309–320.

Ban, Y.H., Xu, Z.Y., Yang, Y.R., Zhang, H.H., Chen, H., Tang, M., 2017. Effect of dark septate endophytic fungus *gaeumannomyces cylindrosporus* on plant growth, photosynthesis and Pb tolerance of maize (*Zea mays* L.). Pedosphere 27, 283–292.

Belldereske, L., Takacsvesbach, C., Kivlin, S.N., Emery, S.M., Rudgers, J.A., 2017. Leaf endophytic fungus interacts with precipitation to alter belowground microbial communities in primary successional dunes. FEMS Microbiol. Ecol. 93 fix036.

Belnap, J., Phillips, S.L., Sherrod, S.K., Moldenke, A., 2005. Soil Biota can change after exotic plant invasion: does this affect ecosystem processes? Ecol. 86, 3007–3017.

Berg, G., Smalla, K., 2010. Plant species and soil type cooperatively shape the structure and function of microbial communities in the rhizosphere. FEMS Microbiol. Ecol. 68, 1–13.

Bipfubusa, M., Angers, D.A., N'Dayegamiye, A., Antoun, H., 2008. Soil aggregation and biochemical properties following the application of fresh and composted organic amendments. Soil Sci. Soc. Am. J. 72, 160–166.

Bizabani, C., Dames, J., 2015. Effects of inoculating *Lachnum* and *Cadophora* isolates on the growth of *Vaccinium corymbosum*. Microbiol. Res. 181, 68–74.

Ding, L.J., Su, J.Q., Sun, G.X., Wu, J.S., Wei, W.X., 2018. Increased microbial functional diversity under long-term organic and integrated fertilization in a paddy soil. Appl. Microbiol. Biot. 102, 1969–1982.

Edwards, J., Johnson, C., Santosmedellín, C., Luriea, E., Podishetty, N.K., Bhatnagarc, S., Eisenc, J.A., Sundaresan, V., 2015. Structure, variation, and assembly of the root-associated microbiomes of rice. P. Natl. Acad. Sci. U. S. A. 112, 911–920.

Fitzpatrick, C.R., Copeland, J., Wang, P.W., Guttman, D.S., Kotanen, P.M., Johnson, M.T.J., 2018. Assembly and ecological function of the root microbiome across angiosperm plant species. P. Natl. Acad. Sci. U. S. A. E1157–E1165.

Hakkeling, R.T.A., Diatta, S., Smaling, E.M.A., 1993. Response of upland rice to soil and hydrological conditions on a footslope in central ivory coast. Geoderma 59, 45–56.

Hardoim, P.R., Andreote, F.D., Reinholdhurek, B., Sessitsch, A., Overbeek, L.S., Elsas, J.D., 2011. Rice root-associated bacteria - insights in community structures across ten cultivars. FEMS Microbiol. Ecol. 77, 154–164.

Inselsbacher, E., Näsholm, T., 2012. A novel method to measure the effect of temperature on diffusion of plant-available nitrogen in soil. Plant Soil 354, 251–257.

Jia, M., Chen, L., Xin, H.L., Zheng, C.J., Rahman, K., Han, T., Qin, L.P., 2016. A friendly relationship between endophytic Fungi and medicinal plants: a systematic review. Front. Microbiol. 7, 906–919.

Kan, J.J., Wang, K., Chen, F., 2006. Temporal variation and detection limit of an estuarine bacterioplankton community analyzed by denaturing gradient gel electrophoresis (DGGE). Aquat. Microb. Ecol. 42, 7–18.

Khan, A.R., Ullah, I., Waqas, M., Shahzad, R., Hong, S.J., Park, G.S., Jung, B.K., Lee, I.J., Shin, J.H., 2015. Plant growth-promoting potential of endophytic fungi isolated from Solanum nigrum leaves. World J. Microb. Biot. 31, 1–6.

Klarner, H., Streck, A., Siebert, H., 2017. PyBoolNet - a Python package for the generation, analysis and visualisation of boolean networks. Bioinformatics 33, 770–772.

Kraigher, B., Mandic, I., 2011. Nitrification activity and community structure of nitrite-oxidizing bacteria in the bioreactors operated with addition of pharmaceuticals. J. Hazard. Mater. 188, 78–84.

Leip, A., Billen, G., Garnier, J., Grizzetti, B., Lassaletta, L., Reis, S., Simpson, D., Sutton, M.A., Vries, W., Weiss, F., Westhoek, H., 2015. Impacts of European livestock production: nitrogen, sulphur, phosphorus and greenhouse gas emissions, land-use, water eutrophication and biodiversity. Environ. Res. Lett. 10, 115004.

Li, Y., Niu, S., Yu, G., 2016. Aggravated phosphorus limitation on biomass production under increasing nitrogen loading: a meta-analysis. Glob. Change Biol. 22, 934–943.

Li, X., Zhou, J., Xu, R.S., Meng, M.Y., Yu, X., Dai, C.C., 2017. Auxin, Cytokinin, and ethylene involved in rice N availability improvement caused by endophyte phomopsis liquidambari. J. Plant Growth Regul. 3, 1–16.

Liang, B., Ma, C., Fan, L., Wang, Y., Yuan, Y., 2018. Soil amendment alters soil physicochemical properties and bacterial community structure of a replanted apple orchard. Microbiol. Res. https://doi.org/10.1016/j.micres.2018.07.010.

Liu, L., 2007. Relative quantitative detection of HLA-G mRNA expression in patients with endometriosis by $2^{-\triangle\triangle CT}$ Method. Chin. J. Birth Health Hered. 15, 25–26.

López, S.M.Y., Sánchez, M.D.M., Pastorino, G.N., Franco, M.E.E., García, N.T., Balatti, P.A., 2018. Nodulation and delayed nodule senescence: strategies of two Bradyrhizobium japonicum isolates with high capacity to fix nitrogen. Curr. Microbiol. 75, 997–1005.

Martínez, O.A., Crowley, D.E., Mora, M.L., Jorquera, M.A., 2015. Short-term study shows that phytate-mineralizing rhizobacteria inoculation affects the biomass, phosphorus (P) uptake and rhizosphere properties of cereal plants. J. Soil Sci. Plant Nut. 15, 153–166.

Nie, J., Yang, Z.P., Zheng, S.X., Liao, Y.L., Xie, J., Xiang, Y.W., 2010. Effects of long-term fertilization on reddish paddy soil quality and its evaluation in a typical double-rice cropping region of China. Chinese J. Appl. Ecol. 21, 1453–1460.

Niu, J., Zhang, W., Ru, S., Chen, X., Xiao, K., Zhang, X., Assaraf, M., Imas, P., Magen, H., Zhang, F., 2013. Effects of potassium fertilization on winter wheat under different production practices in the North China Plain. Field Crop Res. 140, 69–76.

Oksanen, J., Blanchet, F.G., Kindt, R., Peter, R., 2013. Minchin Vegan: Community Ecology Package. R Package Version. 2.0-10. https://CRAN.R-project.org/package=vegan.

Olsen, S.R., Cole, C.V., Wantanable, F.S., 1954. Estimation of Available Phosphorus in Soil by Extraction With Sodium Bicarbonate, vol. 939. USDA, Washinton, DC, pp. 1–19.

Qiu, M., Zhang, R., Xue, C., Zhang, S., Li, S., Zhang, N., Shen, Q., 2012. Application of bio-organic fertilizer can control Fusarium, wilt of cucumber plants by regulating microbial community of rhizosphere soil. Biol. Fert. Soils 48, 807–816.

Rashid, M.I., Mujawar, L.H., Shahzad, T., Almeelbi, T., Ismail, I.M.I., Oves, M., 2016. Bacteria and fungi can contribute to nutrients bioavailability and aggregate formation in degraded soils. Microbiol. Res. 183, 26–41.

Rustad, L.E., Cronan, C.S., 1988. Element loss and retention during litter decay in a red spruce stand i. Revue Canadienne De Recherche Forestière 18, 947–953.

Schloss, P.D., Westcott, S.L., Ryabin, T., Hall, J.R., Hartmann, M., Hollister, E.B., Lesniewski, R.A., Oakley, B.B., Parks, D.H., Robinson, C.J., Sahl, J.W., Stres, B., Thallinger, G.G., Horn, D.J.V., Weber, C.F., 2009. Introducing mothur: opensource, platform-independent, community-supported software for describing and comparing microbial communities. Appl. Environ. Microbiol. 75, 7537–7541.

Siddikee, M.A., Zereen, M.I., Li, C.F., Dai, C.C., 2016. Endophytic fungus *Phomopsis liquidambari* and different doses of N-fertilizer alter microbial community structure and function in rhizosphere of rice. Sci. Rep. 6, 32270.

Sommers, L.E., Nelson, D.W., 1972. Determination of total phosphorus in soils: a rapid perchloric acid digestion procedure. Soil Sci. Soc. Am. J. 36, 902–904.

Su, J.F., Shi, J.X., Huang, T.L., Ma, F., 2016. Kinetic analysis of simultaneous denitrification and biomineralization of novel *Acinetobacter* sp. CN86. Mar. Pollut. Bull. 109, 87–94.

Talapatra, K., Das, A.R., Saha, A.K., Das, P., 2017. In vitro antagonistic activity of a root endophytic fungus towards plant pathogenic fungi. J. Appl. Biol. Biotech. 5, 68–71.

Wang, N., Ding, L.J., Xu, H.J., Li, H.B., Su, J.Q., Zhu, Y.G., 2015. Variability in responses of bacterial communities and nitrogen oxide emission to urea fertilization among various flooded paddy soils. FEMS Microbiol. Ecol. 91 fiv013.

Wei, B., Yu, X., Zhang, S., Gu, L., 2011. Comparison of the community structures of ammonia-oxidizing bacteria and archaea in rhizoplanes of floating aquatic macrophytes. Microbiol. Res. 166 (6), 468–474.

Xu, J., Jia, Z., Lin, X., Feng, Y., 2017. DNA-based stable isotope probing identifies formate-metabolizing methanogenic archaea in paddy soil. Microbiol. Res. 202, 36–42.

Yang, B., Wang, X.M., Ma, H.Y., Jia, Y., Li, X., Dai, C.C., 2014a. Effects of the fungal endophyte *Phomopsis liquidambari*, on nitrogen uptake and metabolism in rice. Plant Growth Regul. 73, 165–179.

Yang, B., Ma, H.Y., Wang, X.M., Jia, Y., Hu, J., Li, X., Dai, C.C., 2014b. Improvement of nitrogen accumulation and metabolism in rice (*Oryza sativa* L.) by the endophyte *Phomopsis liquidambari*. Plant Physiol. Biochem. 82, 172–182.

Yang, B., Wang, X.M., Ma, H.Y., Yang, T., Zhou, J., Dai, C.C., 2015. Fungal endophyte *Phomopsis liquidambari* affects nitrogen transformation processes and related microorganisms in the rice rhizosphere. Front. Microbiol. 6, 00982.

Yoshida, M., Ishii, S., Otsuka, S., Senoo, K., 2010. nirK-harboring denitrifiers are more responsive to denitrification- inducing conditions in rice paddy soil than *nirS*-harboring bacteria. Microbes Environ. 25, 45–48.

Youatt, J.B., 1954. Denitrification of nitrite by a species of Achromobacter. Nature 173, 826–827.

Yu, H., Zhang, L., Li, L., Zheng, C., Guo, L., Li, W., Sun, P., Qin, L., 2010. Recent developments and future prospects of antimicrobial metabolites produced by endophytes. Microbiol. Res. 165 (6), 437–449.

Yuan, Z.L., Dai, C.C., Li, X., Tian, L.S., Wang, X.X., 2007. Extensive host range of an endophytic fungus affects the growth and physiological functions in rice (*Oryza sativa* L.). Symbiosis 43, 21–28.

Zhalnina, K., Louie, K.B., Hao, Z., Mansoori, N., da Rocha, U.N., Shi, S., Cho, H., Karaoz, U., Loqué, D., Bowen, B.P., Firestone, M.K., Northen, T.R., Brodie, E.L., 2018. Dynamic root exudate chemistry and microbial substrate preferences drive patterns in rhizosphere microbial community assembly. Nat. Microbiol. 3, 470–480.

Zhang, J., Zhang, N., Liu, Y.X., Zhang, X., Hu, B., Yuan, Q., Xu, H., Wang, H., Guo, X., Qian, J., Wang, W., Zhang, P., Jin, T., Chu, C., Bai, Y., 2018. Root microbiota shift in rice correlates with resident time in the field and developmental stage. Sci. China Life Sci. 4, 1–9.

Zhou, J., Li, X., Chen, Y., Dai, C.C., 2017. De novo transcriptome assembly of *phomopsis liquidambari* provides insights into genes associated with different lifestyles in rice (*Oryza sativa* L.). Front. Plant Sci. 8, 00121.